Development of GA-based Evolved System for Feedback Control of Turbulence

J. PARK[*], T. YOSHINO[**], T. YAMAGAMI[**], Y. SUZUKI[**] and N. KASAGI[**]

[*]*Institute for Energy Utilization, AIST, 1-2-1 Namiki, Tsukuba-shi, Ibaraki 305-8564, Japan*
[**]*Department of Mechanical Engineering, The University of Tokyo*
7-3-1 Hongo, Bunkyo-ku, Tokyo 113-8656, Japan
E-mail: park@thtlab.t.u-tokyo.ac.jp

This paper introduces recent development of the integrated system for smart control of turbulence. The 3rd generation system inherits the characteristics of the 2nd generation system and improves power consumption, time delay of measuring device, interference by neighboring electromagnet and the sensitivity of the sensor. The 4th generation system is using MEMS actuators which give smaller size and higher productivity. Target Reynolds number can be increased up to 600 due to 1mm spacing of the actuator in spanwise direction. In addition, VLSI controller used in the 4th generation system also has small size but substitute all the instruments including anemometer, DSP board, computer and power amp. These features, MEMS and VLSI, would be a big step toward intelligent skin for turbulence control.

1. INTRODUCTION

In the SMART symposium last year, we presented GA (Genetic Algorithm) based feedback control system with arrayed sensors and actuators which is first generation of our control system[1]. It is composed of wall shear stress sensor, wall deformation actuator, GA based control algorithm and DSP (Digital Signal Processor) based control system. We got 6% reduction of wall shear stress fluctuation at $Re_\tau = 300$ using 24 sensors and 4 actuators. The sensor of first generation system is hotfilm type, fabricated using MEMS technique and has 1mm spanwise spacing. The testing result of arrayed sensor showed a good agreement with DNS data. The actuator of the first generation system is driven by electromagnetic force with silicone rubber membrane and has 4.3mm spanwise spacing. The resonant frequency of the actuator was found to be 600Hz with maximum displacement of 0.25mm, which is enough for turbulence control at the Reynolds number investigated.

The 2nd generation system was developed and tested in a fully developed turbulent channel flow giving 9% reduction of the wall shear stress fluctuation[2]. It uses thermally improved sensors using numerical simulation and smaller actuators – 3.1mm spanwise spacing – and covers larger control area with 192 sensors and 48 actuators. It showed faster convergence than first system (10 generations vs. 100 generations) as well as more reduction rate.

The 3rd generation system has several improvements on the sensor, the actuator and DSP system and is presented in this paper. The sensor is modified from front side contact to back side contact using a novel feed through MEMS technology, which will be explained in more detail later. The improvements on the actuator include minimizing heat transfer to the fluid generated by the coil, shielding magnetic field generated by neighboring electromagnet using Permalloy structures and maximizing electromagnetic force using Permalloy core. A new DSP system is used for third generation system which has faster (0.1ms delay vs. 1.6ms) response than previous one and can measure DC voltage allowing the measurement of averaged wall shear stress.

The 4th generation system is also introduced in this paper, which uses MEMS actuator as well as MEMS sensor. The size of the actuator is reduced to 1mm in spanwise direction, which can be used for the turbulence control at higher Reynolds number up to $Re_\tau = 600$. In addition, VLSI controller

plays important part on the 4th generation system, eliminating huge control system containing computer, DSP system, anemometer and power amp for the actuator.

The 3rd generation system has been fabricated and is being tested in a turbulent channel flow and the result will be presented in the near future. The 4th generation system is under integration and a part of the result on components validation will be presented.

2. CONFIGURATION OF 3rd GENERATION SYSTEM
2.1 Sensor

In the last SMART symposium, we presented hotfilm type wall shear stress sensor developed for turbulence control and thermally optimized using numerical simulation[1]. The simulation revealed that thermal field spreads out in fluid even in the upstream due to heat conduction and inhibits exposure of the hotfilm to the fluid at ambient temperature. It was also found that the hotfilm having slits on both sides shows better performance than that of having vacuum cavity due to the reduction of heat conduction through the substrate. It has been improved using a novel feed through technique which allows backside connection. Due to the wire on the surface, front side connection is supposed to disturb the flow, whereas with backside connection surface around sensor area is flat enough not to influence turbulent flow. The backside connection requires complex fabrication process including silicon D-RIE and glass filling for insulation. Figure 1 shows the photograph of the sensor array where you can see hotfilm sensor, silts around the hotfilm, temperature sensor and pads for back side connection. To demonstrate the performance of the sensor, we tested it in a fully developed turbulent channel and compared it with the result of numerical simulation which is shown in Figure 2. As you can see, the power spectrum of the measured velocity is in good agreement with DNS data at $Re_\tau \sim 650$.

2.2 Actuator

The outlook of the 3rd generation actuator array is shown together with the sensor array in Figure 3, which is almost the same as previous one, but was designed to solve problems on non-uniformity of deformation, power consumption and crosstalk between neighboring actuators which are not negligible in previous one. Figure 4 shows the difference of the new actuator. Permalloy (alloy of Fe & Ni) is used to solve some of problems which has high permeability and is widely used for the application of electromagnet. The crosstalk was significantly suppressed using Permalloy shielding around the electromagnet. Permalloy was also served as a core of a coil, which gives higher electromagnetic force. Power consumption is much reduced as we could reduce the size of the coil and the current due to the higher electromagnetic force described above. In addition, the thickness of permanent magnet could be reduced to half for the same reason that minimizes non-uniformity of deformation. Due to the decrease of mass, dynamic response becomes 40% faster (700Hz) than the previous actuator. We succeeded in designing and fabricating such kind of actuator using the nonlinear magnetic field FEM analyses, ANSYS. The magnetic field strength calculated is shown in Figure 5 and we can see that the most of the magnetic field is confined inside the Permalloy shielding. The measurement of displacement of the new actuator is shown in Figure 6, where power needed to obtain the same displacement is reduced, which means efficiency of the actuator is improved and the heat generation is reduced. We even installed cooler around the actuator to eliminate heat transfer to the fluid completely.

2.3 Control system

A control system of the 3rd generation system is composed of a host computer, DSP board and GA based control algorithm. A new DSP is used for the 3rd generation system and has 192 AD inputs and 64 DA outputs. Time delay of the new DSP including 192 channel AD conversion, data

calculation and 64 channel DA conversion is within 0.1ms. Considering that previous DSP spent 1.6ms for less number of sensors and actuators, total time delay was drastically reduced. In the experiment of drag reduction, GA optimizing program is included in the DSP as well as control algorithm.

3. CONFIGURATION OF 4th GENERATION SYSTEM

Figure 7 shows a schematic diagram of the 4th generation system which is composed of an upstream sensor array, an actuator array and VLSI controller. A flexible cable is used for information exchanging between VLSI and the sensors and the actuators. The sensor is the same as the 3rd generation but the actuator is quite different from previous generations and VLSI control chip is controlling all the components instead of DSP system.

3.1 Actuator

Since DNS predicted significant drag reduction using a virtual actuator[3], experimental realization of active turbulence control has been tried using a variety of actuators including synthetic jet[4], Lorentz force[5], oscillatory blowing[6] and wall oscillation[7]. A wall deformation actuator is one of the most promising actuators because of its simple structure and has been used in many previous researches. Typical wall deformation actuator is composed of membrane which serves as wall and force generating components. We demonstrated wall deformation actuators for turbulence control last year and improved it using MEMS technique.

The 4th generation MEMS actuator is using electromagnetic force to generate wall motion. The electromagnetic force is generated by interaction between magnetic field and the electrical current through a coil and is proportional to magnetic field strength, current and the length of the coil[8]. The range of operating voltage for the actuator depends on the force required to produce wall motion and can be determined by the cross sectional area of the coil. In present application, 3V range was used considering that the maximum voltage of the VLSI is 5V. The current of the coil is 15mA at this voltage. Being able to operate the actuator with relatively low voltage is one of the major advantages of using electromagnetic force.

The size of the actuator in the spanwise direction can be reduced to 1mm due to MEMS technique which was 3mm up to the 3rd generation system. 1mm spacing of the actuator same as that of sensor enables the 4th generation system to have higher special resolution for flow control. In addition, MEMS technique makes it possible to fabricate arrays of actuators more productively. The length of the actuator is 7mm which was determined by the averaged size of the near-wall streamwise vortices.

Figure 8 shows the fabrication process of the MEMS actuator. Metal deposition on a silicon wafer having 0.5μm SiO$_2$ layers is the first process. 15nm titanium layer is for promoting adhesion between silicon wafer and 150nm copper layer which works as a seeding layer for coil electroplating. 1μm Parylene coating is followed for insulation of coil from bridge. Parylene layer is patterned using oxygen plasma to make contacting area with the coil followed by 200nm copper deposition and patterning for the bridge. Finally D-RIE etching from the backside of the wafer releases the actuator from the substrate. The actuator is supported by copper hinge which has 5μm thickness and 20μm width as shown in Figure 9. The hinge can be made by silicon[9] which is much harder but stronger than copper. In other words, we can get higher deformation using the copper hinge. However durability of the copper hinge should be tested before an application.

To get a force in the wall-normal direction, we need magnetic field in the spanwise direction. Using a staggered array of the magnet, strong spanwise magnetic field can be obtained. Figure 10 is the result of simulated magnetic field on the surface 300μm above the magnet using ANSYS.

Minimum value is shown on the center of the magnet and it becomes maximized on the edge of the magnet.

3.2 VLSI controller

To realize embedded controller, MICS (Multi user Integrated Chip Service) was used[10]. The chip is as small as 3.1mm by 3.8mm, and has nine independent blocks and 42 in/out pads. By designing patterns in two metal layers connecting components (transistor, resistor and capacitor) in each block, we can generate a functional unit including amplifier, multiplier, filter, etc. Figure 11 shows circuit diagram of VLSI designed for the flow control. It has sensor controller(block #1), signal amplifier(block #2), linearizer(block #3, #4), GA controller(block #5, #6, #7, #8) and power amplifier(block #9). Each block was simulated using SPICE before fabrication. The sensor controller is a simple bridge amplifier designed for a hotfilm type wall shear stress sensor including bridge offset adjustment. The overheat ratio and the bridge offset of the controller can be adjusted from the outside of the chip. The signal amplifier is using a differential amplifier and the gain is controlled by external resistances. A hotfilm sensor has nonlinear characteristics which is negative for embedded controller, so the linearizer is designed using two squarers. The GA controller is based on a linear control algorithm accepting 3 upstream sensor inputs and generating an output for an actuator. Each input value is multiplied by weighting factor and transferred to adder, where the final control value is produced. The linear algorithm is easy to realize and needs small number of hardware units, but nonlinear controller like neural network is also possible to be embedded in VLSI which has larger number of blocks. The power of the output signal is not high enough for the actuator and the power amplifier can be used for the current amplification up to 30mA. Figure 12 shows the prototype of the VLSI fabricated for the 4th generation system.

4. CONCLUSIONS

Evolved system for GA-based feedback control of turbulence was designed and fabricated. The 3rd generation system has optimized sensor, actuator and control system. The 4th generation system is characterized by MEMS actuator and VLSI controller allowing us to make a very compact system, which is closer to real application than previous system. The 4th generation system is under development and turbulence control at high Reynolds number will be reported in the near future.

REFERENCES

[1] Y. Suzuki, T. Yoshino, and N. Kasaki, Proc. 4th Symp. Smart Control of Turbulence, 2003, pp115-122

[2] T. Yoshino, Y. Suzuki, and N. Kasaki, Proc. 3rd Int. Symp. Turbulence and Shear Flow Phenomena, 2003, pp179-184

[3] H. Choi, P. Moin, and J. Kim, J. Fluid Mech. **262**, 1994, pp75-110

[4] A. Glezer and M. Amitay, Annu. Rev. Fluid Mech. **34**, 2002, pp503-529

[5] C. Henoch and J. Stace, Phys. Fluids **7**, 1995, pp1371-1383

[6] A. Seifert and L. Pack, AIAA J. **37**, 1999, #99-0925

[7] W. Jung, N. Mangiavacchi, and R. Akhavan, Phys. Fluids A **4**, 1992, pp1605-1607

[8] J. Bernstein, W. P. Taylor, J. Brazzle, G. Kirkos, J. Odhner, A. Pareek, and M. Zai, MEMS 2003, pp275-278

[9] H. Miyajima, N. Asaoka, T. Isokawa, M. Ogata, Y. Aoki, M. Imai, O. Fujimiri, M. Katashiro, and K. Matsumoto, MEMS 2002, pp552-555

[10] K. Maenaka, K. Asada, K. Okamoto, T. Fujita, and M. Maeda, Tech. Dig. Of the 16th Sensor Symp., 1998, pp227-230
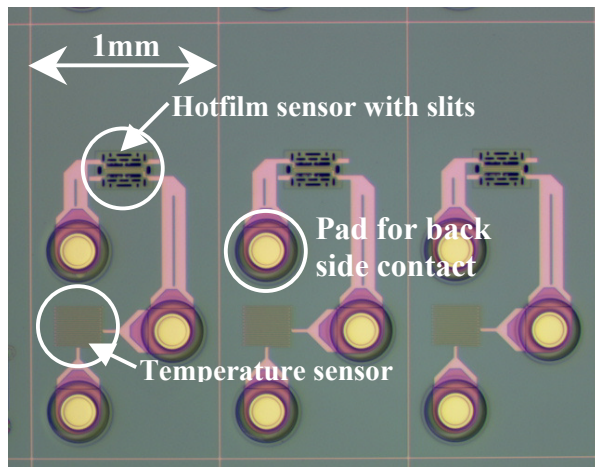
Fig. 1 Photograph of the array of wall shear stress sensor for 3rd and 4th generation 1mm × 2.4mm
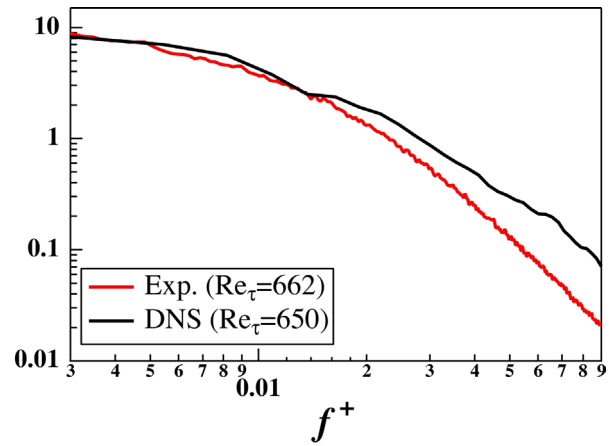

Fig. 2 Comparison of power spectrum of wall shear stress between measured data with the new sensor and DNS result
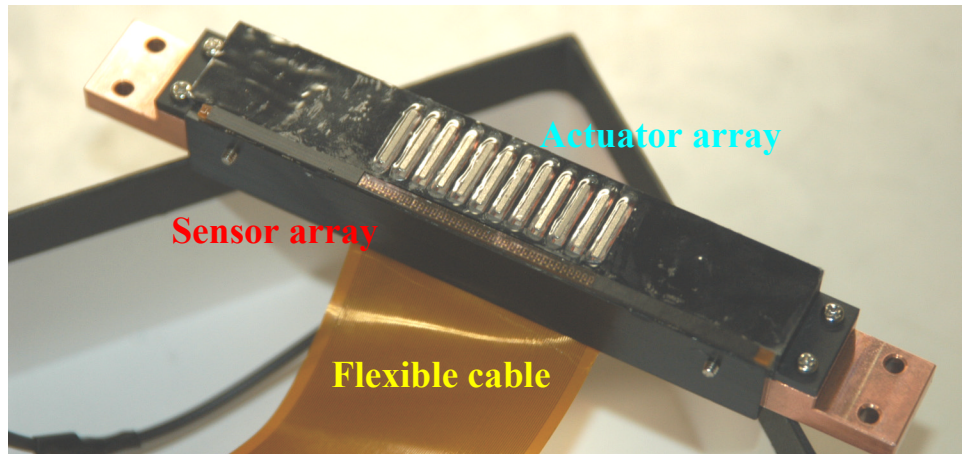

Fig. 3 One row of sensor and actuator unit of 3rd generation system, 7 rows are installed in the turbulent channel for the evaluation
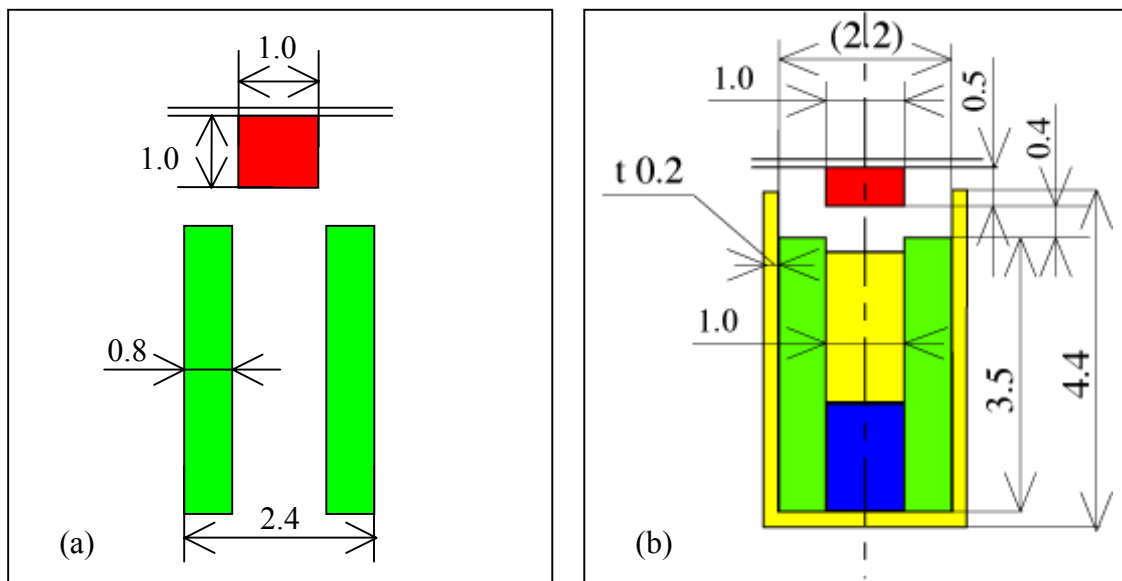

Fig. 4 Schematic diagram of the actuator (a) 2nd generation, (b) 3rd generation
Green is coil, red and blue is permanent magnet and yellow is Permalloy.
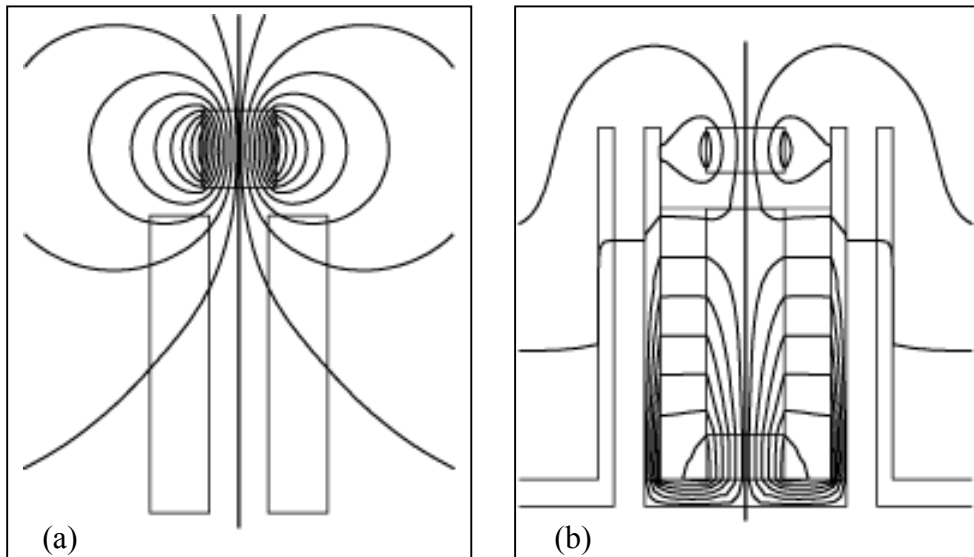
Fig. 5 Contour lines of electromagnetic field strength (a) 2nd generation, (b) 3rd generation
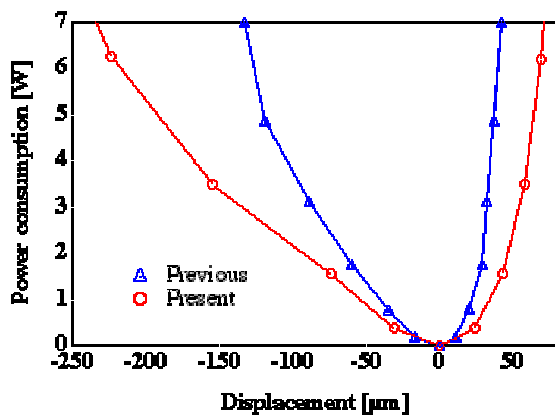
Fig. 6 Measured power consumption of the actuator to obtain wall deformation
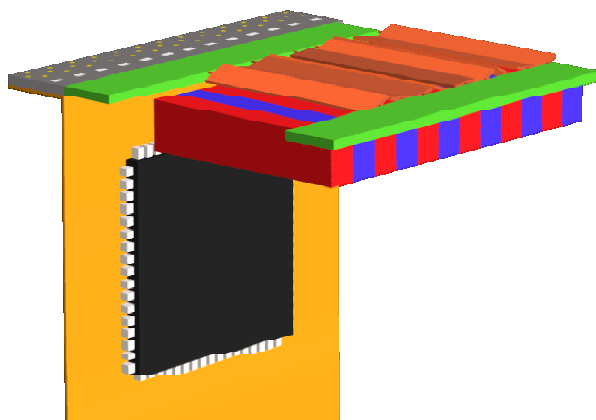

(a) Ti(15nm) & Cu(150nm) deposition & PR(AZP4620 ~ 6mm) patterning

(b) Coil electroplating

(c) Etch seeding layer

(d) Parylene coating(2mm) & patterning(RIE etching)

(e) Cu(150nm) deposition & patterning bridge

(f) Silicon D-RIE

Fig. 7 Schematic diagram of 4th generation system
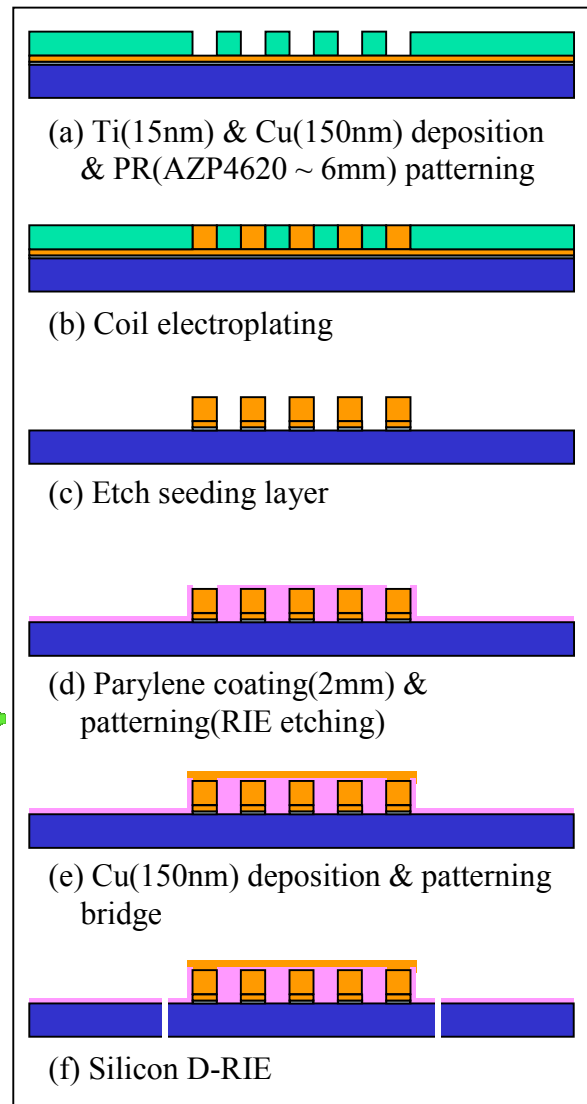
Fig. 8 Fabrication process of 4th generation MEMS actuator
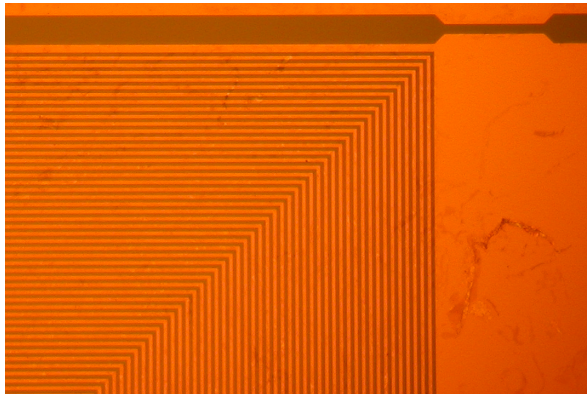
Fig. 9 Magnified view of coil and hinge on the 4th generation MEMS actuator
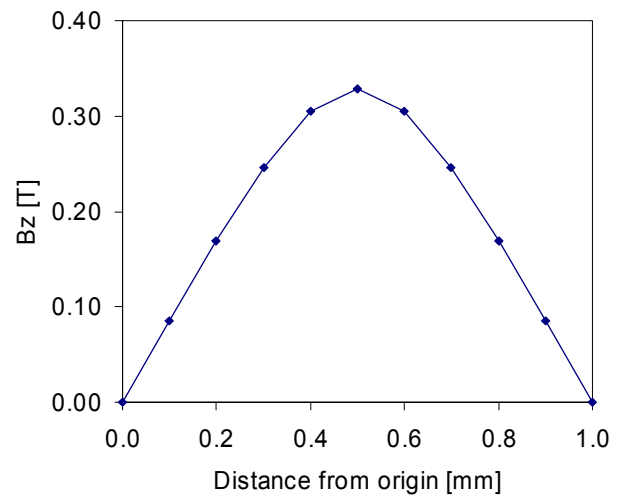

Fig. 10 Calculated magnetic field in spanwise direction at 300μm above the magnet using ANSYS
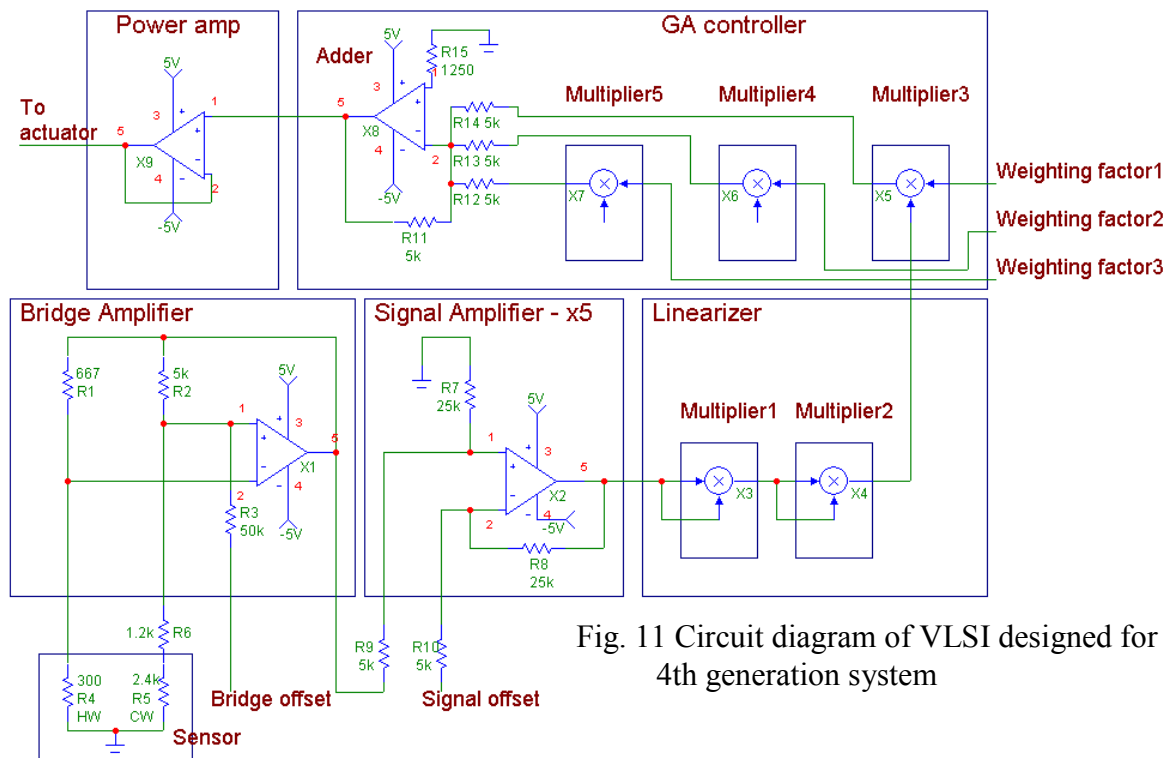

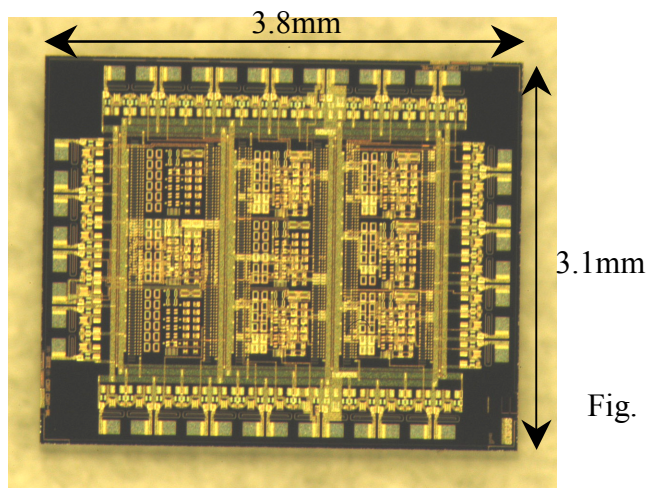Fig. 11 Circuit diagram of VLSI designed for 4th generation system

Fig. 12 Magnified view of VLSI having 9 blocks and 42 in/out pads